This article has been accepted for publication in a future issue of this journal, but has not been fully edited. Content may change prior to final publication. Citation information: DOI 10.1109/TPWRD.2018.2799181, IEEE Transactions on Power Delivery

A Decentralized Fault Detection Technique for Detecting Single Phase to Ground Faults in Power Distribution Systems with Resonant Grounding

M. A. Barik, *Student Member, IEEE,* A. Gargoom, *Member, IEEE,* M. A. Mahmud, *Member, IEEE,* M. E. Haque, *Senior Member, IEEE,* Hassan Al-Khalidi, and AMT Oo, *Member, IEEE*

***Abstract*—This paper presents a decentralized fault detection technique for power distribution systems with resonant grounding (RG). The aim of this paper is to detect single phase to ground (SPG) faults and identify the faulty feeder within three cycles of the fault occurrence. In the proposed technique, faults are firstly detected based on the neutral voltage displacement. The pre-fault and post-fault voltages (phase to ground) are then used to identify the faulty phase. Finally, the faulty feeder (as well as the faulty area of a long feeder) is identified from the relationship between the initial transient of the zero-sequence current and the faulty phase voltage just after the occurrence of faults. A signal processing tool called mathematical morphology (MM) is utilized to identify the faulty feeder. To identify the faulty feeder, it is also required to know the fault occurrence time which is estimated using the slope of the neutral voltage. The main feature of the proposed scheme is that this technique only uses voltage and current signals from the corresponding voltage transformers (VTs) and current transformers (CTs). Therefore, it does not require communication among protection devices in the same or different feeders to identify the faulty feeder. The proposed technique also has the ability to distinguish the nature of faults, i.e., whether the faults are permanent or temporary. The effectiveness of the proposed scheme is tested, on an IEEE test system as well as on a practical test system, using *MATLAB/SimPowerSystems*. Simulation results show that the proposed technique can quickly detect the SPG faults in a RG power distribution system and identify the faulty feeder. It is also capable of distinguishing faults from other disturbances. Moreover, it works under different compensation levels (CLs) as well as for different fault inception angle (FIAs).**

***Index Terms*—Fault detection, low fault current, mathematical morphology, resonant grounding, single phase to ground faults.**

I. Introduction

FAULT detection is a very important issue to consider in power systems to ensure safety, reliability and to avoid accidents, damages to equipment and undesired blackouts. There are several types of faults which can occur in power systems such as SPG faults, phase to phase faults, double phase to ground faults, and three phase to ground faults. Among these faults, the SPG fault is the most common one which is required to be detected so that the faulty section can be isolated as soon as possible [1].

The most common practice of utilities is to use overcurrent relays to detect faults in distribution systems which track the feeder current and indicate a fault if the current is higher than a predefined threshold [2]–[4]. The threshold for over-current relays depends on the load current. Usually, the threshold is set to a little higher than the usual load current of the feeder. However, this technique does not work for the faults where the fault currents are very low as the feeder currents for those faults lie under the threshold level.

On the other hand, the magnitude of fault currents due to ground faults in a power distribution network depend on the grounding practices of distribution substation transformers where fault currents are required to be very low for safety purposes. The neutral point of the substation transformer can be grounded through various ways, e.g., solidly grounded, resistance grounded, ungrounded (isolated), and resonant grounding (RG). Among these grounding practices, RG-based techniques can quickly decrease the fault current (usually three cycles) of SPG faults to a very small level which is mostly independent of fault impedance (FI) [5]. In these cases, the fault currents of ground faults are very small and the conventional overcurrent relays do not work. Thus, a new and improved method is required to detect SPG faults and identify the faulty feeder of RG distribution systems (within three cycles) where fault currents are very low even if the FI is low.

Most of the existing research activities for fault detections are conducted for solidly or resistance grounded systems, i.e., without considering the mechanism of the RG. There are some literature on the detection of high impedance faults (HIFs) [6]–[10] where the fault currents are low, i.e., similar to that of the RG system. An artificial neural network (ANN)-based method is presented in [7] to detect HIFs. The major limitations of the ANN-based method are that it requires a large number of training set and suffers from the computational burden. In [8], a pattern recognition technique is used to detect faults using the sequence component of the current signal where the fault signatures are not unique. Recently, a time frequency-based technique [9] and a mathematical morphology (MM)-based technique [10] are used to detect HIFs. These approaches mainly focused on the fault detection. However, the behaviors of the entire system will change during ground faults in a RG system. Therefore, it is also important to identify the faulty feeder and/or the specific area of a feeder where fault occurs. Moreover, the fault characteristics of the RG system are different from the fault characteristics of a solidly grounded system. For example, the fault currents are very small for both HIFs and low impedance faults (LIFs) when there exist ground faults in a RG system where the fault currents are small only for HIFs in the solidly grounded system.

There are some available approaches which have the ability to detect different faults in RG power distribution systems. A fault detection method is presented in [11] for detecting low current faults in distribution systems which work for any type of grounding practice, e.g., RG, solidly grounded, and resistance grounded. In this method, a voltage signal of a certain frequency other than the fundamental frequency is superimposed in the substation bus. An asymmetry is then calculated in [11] to identify the faulty

M. A. Barik, A. Gargoom, M. A. Mahmud, M. E. Haque, and AMT Oo are with the Electrical Power and Energy System Research Lab, School of Engineering, Deakin University, Geelong, Australia. Emails: mbarik@deakin.edu.au, a.gargoom@deakin.edu.au, apel.mahmud@deakin.edu.au, enamul.haque@deakin.edu.au, and aman.m@deakin.edu.au

Hassan Al-Khalidi is with AusNet Services, Melbourne, Australia. Email: Hassan.Al-Khalidi@ausnetservices.com.au

This research work is fully funded by AusNet Services, Melbourne, Australia (Grant number: RM000003126).

This article has been accepted for publication in a future issue of this journal, but has not been fully edited. Content may change prior to final publication. Citation information: DOI 10.1109/TPWRD.2018.2799181, IEEE Transactions on Power Delivery

feeders and phases from residual currents, neutral voltages, and phase voltages in three different stages (pre-fault, superposition, and fault situations). However, the performance of this method depends on the accuracy of the residual current measurement. An improvement of [11] is made in [12] where phase currents are used instead of residual currents to calculate the phase and feeder asymmetries which enhance the overall performance. However, the approach in [12] requires communication among feeders to identify the faulty feeders especially for detecting faults in the field level as the field devices are far away from each other. Also, the inclusion of an additional voltage signal with a different frequency can have some other effects (e.g., signal attenuation) to the system.

Another fault detection method which uses the grey relation degree of zero-sequence currents to identify the faulty feeder in a RG system is presented in [13]. In this technique, the degree of relationship between zero-sequence currents in different feeders is calculated to distinguish faulty and healthy feeders. This method works well for at least three feeders' substations as it requires a minimum number of three feeders to calculate the degree relationship between feeders which limits the applicability. Moreover, this approach works based on the communication among protection devices.

An impedance-based fault detection technique is presented in [14] where the faulty feeder is identified by comparing the calculated line to ground impedance of each feeder. In this method, the up-to-date information of line to ground susceptance value is always required in the supervisory control and data acquisition (SCADA) to identify the faulty feeder. For example, it is required to update the susceptance value in the SCADA if a small section get connected/disconnected to/from the network which is very common during the operation of power networks. Moreover, this technique mainly focuses on the fault detection in the substation level without any indication of its ability to work in the filed. Even if this method will work in field level, it will require communication between feeders to identify the faulty feeder as this technique identify the faulty feeder by comparing the line to ground impedance of all feeders.

From the existing literature on the fault detection of power distribution systems with RG, it is clear that these approaches are designed to serve some specific purposes. The common drawback associated with most of the existing methods for fault detections of power distribution systems with RG is that these require a communication link among different protection devices in order to detect the fault. Though there have been lots of improvements on the communication schemes in power systems in recent years, the reliability of fault detection is significantly affected in the case of unexpected events, e.g., communication failures or delays. The problem of communication among different devices can be resolved by designing a fault detection scheme which uses only local information, i.e., by proposing a decentralized scheme.

This paper proposes a decentralized fault detection algorithm to detect SPG faults in power distribution systems with RG. The proposed algorithm detects the faults within power distribution systems with RG using the neutral voltage displacement while fault occurrence time is estimated using the slope of the neutral voltage as this is important to identify the faulty feeder. After detecting faults, the faulty phase is identified by comparing the pre-fault and post-fault phase voltages. This technique identifies the faulty feeder based on the relationship between the initial transient of the zero-sequence current and the voltage of the faulty phase just after the occurrence of a fault. In this case, a signal processing technique called mathematical morphology (MM) is used to track the transient of the zero-sequence current. The natures of faults (temporary or permanent) are also identified using the neutral voltage displacement. The main contribution of this paper is to identify the faulty feeder in a RG power distribution system for a SPG fault. The superiorities of the proposed fault detection method are clarified through the following key points:

- Ability to identify the faulty feeder without any communication among circuit breakers (CBs) and auto circuit reclosers (ACRs) on the other sections of the same or other feeders.
- Ability to localize the faulty area of a long feeder.
- No dependency on the number of the feeders in the substation as this is decentralized and each protection device independently detects faults.
- All voltages and zero-sequence current data are only used in this technique which are usually available in the measurement and does not use any system parameter which might change frequently in the real system.
- Ability to detect fault and identify the faulty feeder within 15 ms.

II. Effects of Resonant Grounding Technique on Fault Detection

RG is a way to ground the neutral of distribution substation transformer with a variable inductance coil which is known as arc suppression coil (ASC). A power distribution system with RG is shown in Fig. 1 where an ASC is connected between the neutral point of the substation transformer and the ground. Also, the ASC is connected to a neutral management system (NMS) which controls the ASC to achieve resonance with the system's zero-sequence impedance based on voltage and current information from both neutral point and the feeders' instrument transformers, i.e., CTs and VTs. Here, the ASC minimizes the fault current to a very low value.

To validate the above statement, a fault is simulated on the IEEE 13 node test system with and without RG (solidly grounding). In both cases, a SPG fault with a FI of $10\ \Omega$ is applied at the same location of the test system. The fault currents from the simulation are shown in Fig. 2 from where it is clear that the RG reduces the fault current for the SPG fault to a very small value. Therefore, it is obvious that RG can compensate the fault current

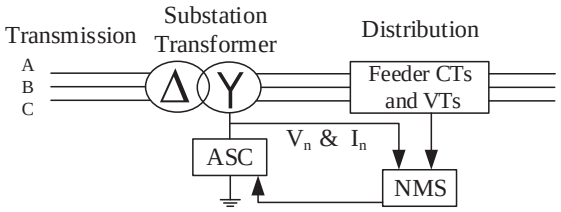

Fig. 1: A distribution substation with resonant grounding.

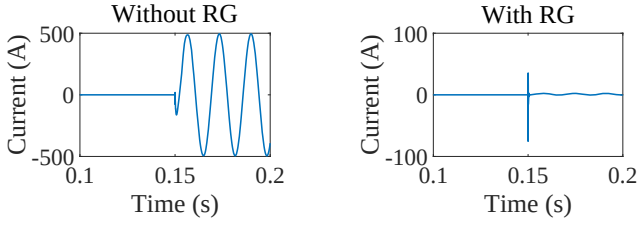

Fig. 2: Fault currents with and without resonant grounding.

This article has been accepted for publication in a future issue of this journal, but has not been fully edited. Content may change prior to final publication. Citation information: DOI 10.1109/TPWRD.2018.2799181, IEEE Transactions on Power Delivery

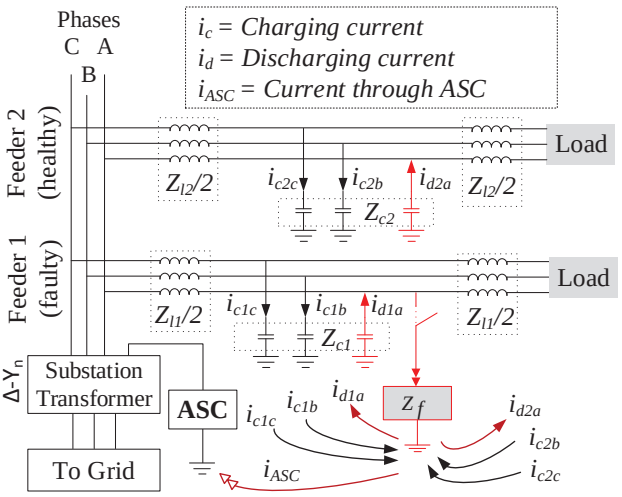

Fig. 3: Equivalent circuit diagram of a resonant grounded power distribution system with a single phase to ground fault.

for SPG faults. As the fault detection methods based on overcurrent are not capable of detecting SPG faults of the resonant grounded system, this paper proposes a fault detection technique where the fault detection is done using the neutral voltage displacement. In this method, every CB and auto circuit ACR see all faults that occur in the system as the neutral voltage of the entire system is almost the same. Therefore, the initial transient behavior of the zero-sequence current is used to identify the faulty feeder and/or a specific area of a large feeder where the fault occurs. The proposed fault detection technique is described in the following sections.

III. Fault Detection

In RG power distribution systems, the fault currents are very small for SPG faults where the changes in neutral voltage are significant. Thus, the neutral voltage displacement is utilized in the proposed technique to detect SPG faults which is discussed in this section. Also, a technique for estimating fault occurrence time is developed which is required to identify the faulty feeder as presented in Section V. The fault occurrence time is defined as the time when a fault occurs which is essential to estimate as it may take time to detect faults. In addition, a technique is proposed to find out the nature of a fault whether it is permanent or temporary. The details are discussed in the following subsections.

A. Fault Detection

In the event of SPG faults in a RG system, an unbalance creates between phase voltages which increases the neutral voltage. To explain this scenario, a distribution system with two feeders is shown in Fig. 3 where a SPG fault is applied on phase *A* of feeder 1. In this case, although the resultant fault current is close to zero due to resonance, the voltages will follow the Kirchhoff's Voltage Law (KVL). A simplified circuit for the faulty phase is shown in Fig. 4 where the neutral to ground voltage (V_n) during the fault can be expressed as:

$$V_n = \frac{Z_{ASC}}{Z_{ASC} + Z_l + Z_c \| Z_f} V_{pn} \tag{1}$$

where Z_{ASC} is the impedance across ASC, Z_l and Z_c are the inductive and capacitive impedances of the distribution line, respectively, Z_f is the FI, and V_{pn} is the phase to neutral voltage. On the other hand, for the healthy condition V_n is:

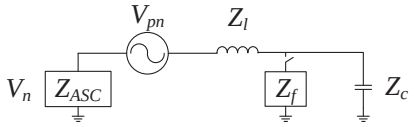

Fig. 4: Equivalent circuit for the faulty phase.

$$V_n = \frac{Z_{ASC}}{Z_{ASC} + Z_l + Z_c} V_{pn} \tag{2}$$

From these equations, it can be seen that the neutral voltage of the system will increase during a fault as $Z_c \| Z_f < Z_c$. Therefore, the neutral to ground voltage can be used to detect ground faults where the fault is indicated by the neutral voltage exceeding a set threshold. Here, the threshold for neutral voltage is different for every system and depends on the system parameters such as system unbalance.

Moreover, the neutral voltage might vary with any changes in the loads in the system or ungrounded shunt capacitor bank (USCB) switching. In a RG distribution system, loads are usually connected between phases. Thus, the load currents do not have the component which flows through the ground path. Similarly, USCBs do not have any ground path. However, the phase voltages can vary with the load changes (LCs) or USCB switching which can change the residual current in normal condition. Also, the variation in residual current can change the neutral voltage which is negligible as the changes in voltages are not significant due to the load variation or USCB switching. In addition, the neutral voltage changes due to the network capacitive unbalance as it can cause residual current to flow. The capacitive unbalance can be caused by the unequal lengths and different types of conductors between phases of the distribution lines. For example, the level of network capacitive unbalance can change due to cut-off a section. Therefore, capacitive balancing will be required to minimize the residual current which is beyond the scope of the paper.

B. Estimation of Fault Occurrence Time

In the previous subsection, the technique to detect faults based on the neutral voltage displacement is explained. However, it may takes time to detect the fault as the neutral voltage crosses the threshold after a time delay. This time delay depends on the dynamics of the system as well as FI. In this case, the slope of the neutral voltage is used to estimate fault occurrence time as the slope of the neutral voltage is steep at the time of a fault. Therefore, if the slope of the neutral voltage is steeper than a set value and continues until the neutral voltage crosses its threshold, the time of starting point where the slope becomes steep can be considered as the fault occurrence time. In the proposed technique, the accuracy to estimate the fault occurrence time will be high as this algorithm uses the slope of the neutral voltage where the slope is usually steep just after the fault occurrence time.

C. Identification of Fault Characteristics

After detecting a fault, an important task is to identify the nature of the fault as there are possibilities of either temporary or permanent faults. As discussed in the previous subsection, the neutral voltage is high during the fault. Also, from equations (1) and (2), it is seen that voltage will return to the normal value after the fault is cleared. Thus, if the magnitude of the neutral to ground voltage exceeds a set threshold (V_{th}) and persists for a specified period above this threshold, the fault can be defined as a permanent fault. However, the characteristics of the intermittent

This article has been accepted for publication in a future issue of this journal, but has not been fully edited. Content may change prior to final publication. Citation information: DOI 10.1109/TPWRD.2018.2799181, IEEE Transactions on Power Delivery

arc faults might differ from other SPG faults as the intermittent arcing faults are HIFs with variable FIs during the period of a fault. As a result, the neutral voltage during arc faults is low and oscillates frequently. Sometimes the neutral voltage can go under the threshold during the fault. As a result, some permanent arc faults can be identified as temporary faults. Therefore, the average value of the neutral voltage (during a specific time period) can be used to identify the characteristics of arc faults. The values of V_{th} and period for identifying the permanent fault are usually set by electricity distribution companies based on their best practices. In this case, the period for identifying the characteristics of permanent arc faults and other faults will be different where it will be several times higher for arc faults. The details to identify the characteristic of non-arc and arc fault are discussed in section VI.

IV. Identification of Faulty Phase

After detecting a permanent fault, it is important to find the faulty feeder or the area of a large feeder to isolate the faulty area from the remaining healthy system. There is no need to take any action for the temporary faults as it is cleared by itself. However, it is essential to identify the faulty phase before identifying the faulty feeder in the proposed technique which is discussed in this section.

During the SPG faults in a RG system, the electrical charge of the faulty phase discharges through the phase to ground capacitance of the same phase. From Fig. 3, it can be seen that the voltage of the faulty phase (phase A) discharges through the FI and the phase to ground capacitance of the same phase (i.e., phase A) of all feeders. On the other hand, the charging currents flow from healthy phases (i.e., phases B and C) to faulty phase through the phase to ground capacitance of the healthy phases and the FI. Thus, the phase to ground voltages change and settle down to different values where the voltages of faulty phases reduce to lower values and the voltages of healthy phases increase to a higher value. Therefore, the faulty and healthy phases can easily be identified by calculating the deviation of the RMS value of phase to ground voltages (ΔV_p) as follows:

$$\Delta V_p = V_p(t_f^+) - V_p(t_f^-) \tag{3}$$

where, $V_p(t_f^+)$ and $V_p(t_f^-)$ are the RMS value of post-fault and pre-fault phase to ground voltages, respectively, and t_f is the fault occurrence time. The values of ΔV_p will be negative for faulty phases whereas these values will be positive for healthy phases. Therefore, the faulty phase is identified using ΔV_p.

V. Identification of Faulty Feeder

Although faults can easily be detected by using the neutral voltage displacement, the identification of faulty feeders or a specific area of long feeders where faults are occurred, is challenging. The proposed methodology to identify the faulty feeder is described in this section. Firstly, a mathematical analysis to find out fault signature is explained. Then, the proposed technique to identify the faulty feeder using MM is presented.

A. Fault Signature

To identify the faulty feeder, the characteristics of faulty and healthy feeders during a SPG fault are required to identify first which is discussed in this subsection. At the very first instance of fault occurrence, the current flowing through the fault location (FL) depends on the voltage at the FL and the FI. Therefore, the fault current (i_f) flowing through the faulty feeder at the first instance of fault can be expressed as:

$$i_f = \frac{V_f \sin(\omega t + \delta_v)}{z_f} \quad \text{for } (t - t_f) \gtrapprox 0 \tag{4}$$

$$\Rightarrow I_f \angle \delta_i = \frac{V_f \angle \delta_v}{Z_f \angle \delta_z} \quad \text{for } (t - t_f) \gtrapprox 0 \tag{5}$$

where $v_f = V_f \angle \delta_v$ is the voltage at the FL, $i_f = I_f \angle \delta_i$ is the fault current, and $z_f = Z_f \angle \delta_z$ is the FI. Since, the FI is usually resistive, $\delta_z \approx 0$. Therefore, it can be written from equation (5) as:

$$\delta_i \approx \delta_v \quad \text{for } (t - t_f) \gtrapprox 0 \tag{6}$$

Therefore, it can be concluded from equations (4)-(6) that the polarity of the instantaneous faulty phase voltage of the faulty feeder and the fault current will be same at the FL. Moreover, a significant part of this fault current flows through the zero-sequence path as this is a ground fault. Thus, the zero-sequence current of the feeder will change accordingly when the fault occurs. Therefore, it can be concluded that the change of zero-sequence current through the faulty feeder at the instant of fault occurrence will have the same polarity to that of the instantaneous voltage of the faulty phase.

On the other hand, it can also be seen from Fig. 3 that two feeders are parallel to each other, as well as the phase to ground capacitances of each feeder are parallel to each other. Moreover, the phase to ground capacitors are the major paths to flow the zero-sequence current. This clearly indicates that if the impedance of any parallel branch is suddenly reduced, the currents flowing through the corresponding branch will increase while through other branches will decrease at the very first instance, i.e., before compensating these currents by the source. At the time of faults, the phase to ground impedance of the faulty feeder will be very small. Thus, the zero-sequence current of the faulty feeder will increase while it will decrease for the healthy feeder. This can easily distinguish the changes in zero-sequence currents through the faulty and healthy feeders are opposite to each other.

Finally, it can be concluded that the polarity of the deviation of the zero-sequence current through the faulty feeder will be the same as the instantaneous voltage of the faulty phase voltage while it will be opposite for healthy feeder. This will also be true for the intermittent arc faults as the initial transients are same for both arc and non-arc faults. In this case, the deviation of the zero-sequence current (Δi_0) can be expressed as:

$$\Delta i_0 = i_0(t_f^+) - i_0(t_f^-) \text{ for } (t_f^+ - t_f) \gtrapprox 0 \text{ and } (t_f - t_f^-) \gtrapprox 0 \tag{7}$$

where $i_0(t_f^+)$ and $i_0(t_f^-)$ are the post-fault and pre-fault zero-sequence current (instantaneous values), respectively. A technique to identify the faulty feeder based on this fault signature using MM is developed in the following subsection.

B. Identification of Faulty Feeder Using Mathematical Morphology

From the previous discussion, it can be clearly seen that it is required to track the change of direction for zero-sequence currents at the time of fault occurrence. A signal processing tools called MM is used in this paper to track the change of direction of zero-sequence currents. The MM was first developed by Matheron and Serra [15], [16] based on integral geometry for processing

This article has been accepted for publication in a future issue of this journal, but has not been fully edited. Content may change prior to final publication. Citation information: DOI 10.1109/TPWRD.2018.2799181, IEEE Transactions on Power Delivery

time-domain signals. This is a very useful tools for reshaping time-domain signals which is widely used in image and signal processing fields for de-noising signals or other similar purposes. In power systems, MM is usually used to detect the transient or any unusual change of power system signals [10]. The two fundamental operations of MM are dilation and erosion. For the MM application to detect transients in power system signals, dilation and erosion can be mathematically expressed as [10]:

$$y_d(n) = (f \oplus g)(n) = \max[f(n-m) + g(m)] \quad (8)$$
$$\text{for } (n-m) \geq 0 \text{ and } m \geq 0$$
$$y_e(n) = (f \ominus g)(n) = \min[f(n+m) - g(m)] \quad (9)$$
$$\text{for } (n+m) \geq 0 \text{ and } m \geq 0$$

where $y_d(n)$ and $y_e(n)$ are the dilation and erosion operations outputs of the signal $f(n)$ after processing by a structuring element (SE) $g(m)$, respectively. The SE is a signal processing function by which the signal processing is performed with the MM [10], [17]. In equation (9), few points after the current point are used to analyze a signal, which incurred a time delay. It can be overcome by using the value which is already in the SCADA system instead of using the value of the next few points of the signal. Finally, the dilation and erosion operation can be modified for archiving the better performance to detect any change of a signal in power systems as:

$$y_d(n) = (f \oplus g)(n) = \max[f(n-m) + g(m)] \quad (10)$$
$$\text{for } (n-m) \geq 0 \text{ and } m = 0, 1, 2, ..., l_d$$
$$y_e(n) = (f \ominus g)(n) = \min[f(n-m) - g(m)] \quad (11)$$
$$\text{for } (n-m) \geq 0 \text{ and } m = 0, 1, 2, ..., l_e$$

where l_d and l_e are the length of the SE for the dilation and erosion, respectively. Here, l_d and l_e must be two or more to detect changes in a signal where the maximum length of the SE is not recommended to use very high as it increases the computational burden.

The opening and closing are another two hybrid operations which are based on fundamental operations. The opening ($y_o(n)$) represents dilation operation after the erosion operation and the closing ($y_c(n)$) represents erosion operation after the dilation operation which can be expressed mathematically as [10]:

$$y_o(n) = (f \circ g)(n) = (y_e \oplus g)(n) = ((f \ominus g) \oplus g)(n) \quad (12)$$
$$y_c(n) = (f \bullet g)(n) = (y_d \ominus g)(n) = ((f \oplus g) \ominus g)(n) \quad (13)$$

Another operation called the closing opening difference operation (CODO) which can be used to detect the transient of a signal which can be defined by [10]:

$$y_{CODO}(n) = y_c(n) - y_o(n) \quad (14)$$

where $y_{CODO}(n)$ is the CODO output of $f(n)$. In this case, for detecting the direction of change of a signal, the length of SE has to be different for dilation and erosion operations. Also, the lengths of the SE for opening (l_o) and closing (l_c) have to be the same and equal to either the length of the SE for the dilation or erosion. Otherwise, y_{CODO} will be approximately zero for any transient if the lengths of SE for all operations are the same. Additionally, the lengths of the SE for the dilation, erosion, opening, and closing need to satisfy the following conditions for detecting the change in a specific direction: a) positive (upward) direction: $l_o = l_c = l_d < l_e$ and b) negative (downward) direction: $l_o = l_c = l_e < l_d$.

For detecting changes in both directions, it is required to use two different algorithms in parallel. Therefore, the CODO operation for detecting changes in both direction ($y_{CODOb}(n)$) can be written as:

$$y_{CODOb}(n) = y^{+ve}_{CODO}(n) + y^{-ve}_{CODO}(n) \quad (15)$$

where $y^{+ve}_{CODO}(n)$ and $y^{-ve}_{CODO}(n)$ are the CODO outputs for detecting changes in positive and negative directions, respectively. Using (15), the CODO output of zero-sequence current signals can be used to detect the direction of change of zero-sequence current where a positive spike represents the change in positive direction and a negative spike represents the change in negative direction. However, using a single CODO may give a false result due to measurement errors. Therefore, few CODO outputs can be accumulated to increase the accuracy. On the other hand, the change of the direction of zero-sequence current depends on the sign of the instantaneous value of the faulty phase voltage. Thus, equation (15) can be modified to identify the faulty feeder as:

$$F_{CODO}(t_{fe}) = V_f^{sign} \sum_{t_{fe}}^{t_{fe}+t_r} y_{CODOb}(i_0(t)) \quad \text{for } t_r \gtrapprox 0 \quad (16)$$

where $F_{CODO}(t_{fe})$ is the CODO output of zero-sequence current at t_{fe} for identifying the faulty feeder, v_f^{sign} is the sign of the instantaneous fault voltage at t_{fe} and t_r is the time range to consider y_{CODOb} for identifying faulty feeder after a fault is detected. Here, t_r should be very small (usually two to three samples only) otherwise the signal of zero-sequence current can start changing to opposite direction. Finally, the feeder can be identified as a faulty feeder if a positive spike in the F_{CODO} output appears and healthy for the negative spike. In this case, the CODO operation can only be performed once if a fault is detected. In the following section, the step by step process to detect faults and identify the faulty feeder is explained.

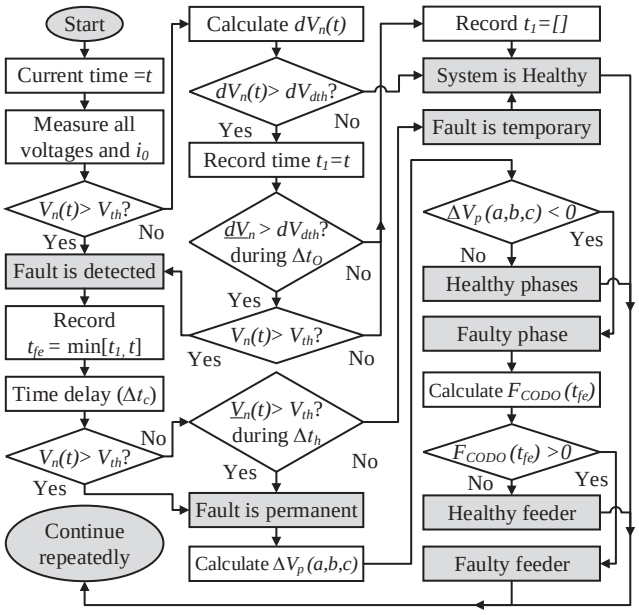

Fig. 5: Flowchart of the proposed fault detection technique.

This article has been accepted for publication in a future issue of this journal, but has not been fully edited. Content may change prior to final publication. Citation information: DOI 10.1109/TPWRD.2018.2799181, IEEE Transactions on Power Delivery

VI. Fault Detection Algorithm

In the proposed method, the SPG fault is detected through several steps. The detailed process for detecting a fault along with the identification of fault characteristics, faulty phase and faulty feeders using the proposed method is presented in Fig. 5. At first, all voltages and the zero-sequence current of the syste/m are measured. The neutral voltage V_n is then compared with the corresponding voltage threshold to detect faults. If V_n is greater than the threshold, the system is identified as a faulty system. Otherwise, the proposed scheme calculates the slope of the neutral voltage (dV_n) and checks whether it is more than a set value dV_{dth} (threshold for the slope) or not. Here, the accuracy of estimating the fault occurrence time will depend on dV_{dth} where the smaller value of dV_{dth} will give better accuracy. However, the very small value of dV_{dth} can be mixed up with the systems usual transients. If $dV_n < dV_{dth}$, it indicates that the system is healthy. Otherwise, this algorithm records current time as t_1 and checks dV_n again for the time duration of Δt_0 (usually few milliseconds) to confirm whether it is a fault or other disturbances. If the average value of the slope of the neutral voltage ($\underline{dV}_n$) is greater than dV_{dth} during the period of Δt_0, this algorithm again checks the V_n. If the average value of dV_n is less than dV_{dth} or V_n is less than V_{th}, this algorithm indicates that the system is healthy and clears the value of t_1. Otherwise, this algorithm will indicate that the system is faulty. After detecting a fault, the fault occurrence time will be estimated and recorded as $t_{fe} = \min[t \;\; t_1]$.

After detecting a fault, it is essential to identify the characteristics of the fault. The first step to identify the fault characteristics is to compare the V_n with V_{th} after a time delay of Δt_c to check whether the fault is permanent or temporary. If $V_n > V_{th}$, the fault will be identified as a permanent fault. However, some permanent intermittent arcing faults may not be detected as the neutral voltage of arcing faults can go below the threshold during a fault. Therefore, again the average value of neutral voltage ($\underline{V}_n$) during another period of Δth (from $t_{fe} + \Delta tc$ to $t_{fe} + \Delta tc + \Delta th$) will be compared with the threshold. If $\underline{V}_n$ exceeds the threshold, it will be identified as a permanent fault, otherwise, the fault will be identified as a temporary fault.

Once a permanent fault is detected, it is required to identify the faulty phase and faulty feeder. To identify the faulty phase, the deviation of all phase voltages at the time of fault occurrence will be calculated using (3). If the deviation of a phase voltage is negative it will be identified as a faulty phase and others are healthy. After identifying the faulty phase, $F_{CODO}(t_{fe})$ of the zero-sequence current will be calculated using (16). If the $F_{CODO}(t_{fe})$ is positive, the feeder will be identified as a faulty feeder, otherwise healthy. This process will continue repeatedly until the feeder is tripped due to a permanent fault. In this case, the identification of the fault characteristics and faulty feeder (including faulty phase) can run in parallel to speed up the detection process. The details simulation results are discussed in the following section.

VII. Results and Discussion

Simulation studies are performed on two test systems (including a practical distribution system) to verify the proposed algorithm. Simulations are conducted in *MATLAB/SimPowerSystems* to get the fault signals and fault signals are analyzed by using the proposed algorithm to detect faults including the identification of fault characteristics, faulty phase, and faulty feeder. In this case,

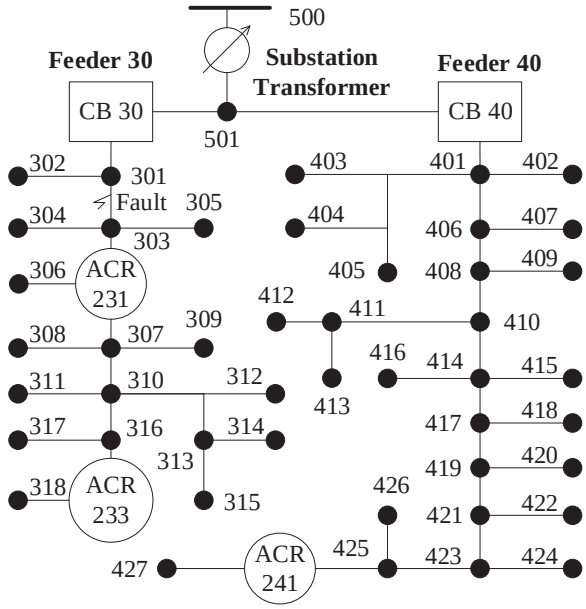

Fig. 6: A practical test system.

the *MATLAB/SimPowerSystems* model of the practical distribution system has been verified with some real measurements. On the other hand, the RG devices are connected to the distribution transformer which will be disconnected if the distribution system is disconnected from the grid (islanding mode). Therefore, it is considered in this paper that the RG systems are grid-connected. The following subsections demonstrate the ability of the proposed algorithm for both test systems under different case studies.

A. Performance Analysis on A Test System Based on A Practical Power Distribution System

A medium voltage $(22\ \mathrm{kV})$ test system based on a practical distribution system as shown in Fig. 6 is simulated to analyze the SPG faults with the proposed fault detection technique. In this simulation, it is considered that all loads are connected between phases but not grounded as the simulations are performed for the RG system where the loads are usually not grounded. The simulations are performed by considering SPG faults with different characteristics (e.g., temporary or permanent). Moreover, the proposed algorithm also distinguishes the faults from other disturbances (such as LCs and USCB switching) which are also verified in this subsection.

1) Distinguishing faults from other disturbances and setting the threshold of the neutral voltage to detect faults: In the proposed framework, faults are detected based on the neutral voltage displacement. Although, the neutral voltage varies due to LCs or USCB switching and ground faults, these changes are small for LCs and USCB switching while high for ground faults. Therefore, it is essential to set a threshold to detect SPG faults. For this purpose, simulations are carried out on the test system as shown in Fig. 6 by applying SPG faults (at phase *A*) with different FIs. The FL is clearly indicated in Fig. 6 which is between node-301 and node-303. Also, the USCB switching is considered on feeder 40 between node-410 and node-414. Moreover, the changes in loads are considered throughout the system and all these information are used to find out the threshold of the neutral voltage.

At first, the neutral voltage is observed with changes in loads and USCB switching where it is considered that the LC occurs at $0.1\ \mathrm{s}$. The changes in loads are considered from 4% to 11%. Also, the

This article has been accepted for publication in a future issue of this journal, but has not been fully edited. Content may change prior to final publication. Citation information: DOI 10.1109/TPWRD.2018.2799181, IEEE Transactions on Power Delivery

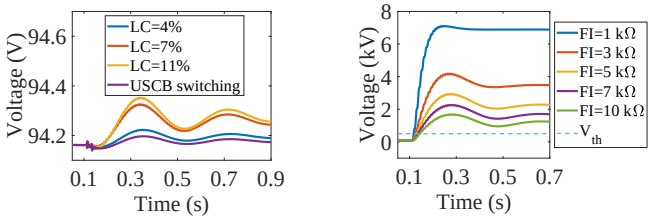

(a) (b)

Fig. 7: Neutral voltages (RMS value) for a) load changes and USCB switching and b) single phase to ground faults.

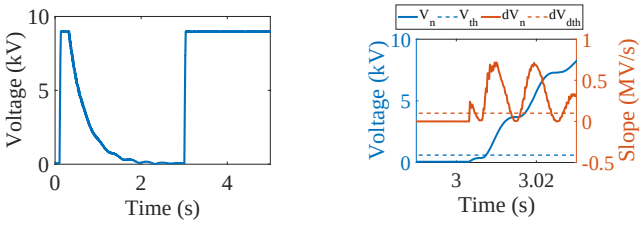

(a) (b)

Fig. 8: a) Neutral voltage (RMS value) for a temporary and a permanent single phase to ground faults and b) neutral voltage (RMS value) and the slope of the neutral voltage for the transient period of the permanent fault.

USCB switching (rating of phase *A*: 100 kVAr, phase *B*: 130 kVAr, and phase *C*: 110 kVAr) is considered at 0.1s. For changes in loads and USCB switching, the neutral voltage is changed which can clearly be seen in Fig. 7a. From Fig. 7a, it can also be seen that the changes in the neutral voltage are not much high.

Now, the neutral voltage is observed by applying SPG faults between node-301 and node-303 with different FIs at 0.1 s. After the fault, the magnitude of the neutral voltage is changed and the changes are higher for the LIFs while these will be lower for HIFs. From Fig. 7b, it can be seen that the neutral voltage is significantly higher when the FI is 1 kΩ. At the same time, the changes in the neutral voltage are lower for a FI of 10 kΩ which can be categorized as a HIF.

Therefore, it is clear from Fig. 7 that the changes in neutral voltage are slightly higher for the changes in loads and USCB switching while the neutral voltage changes much more for single-phase ground faults. From Fig. 7b, it is also obvious that the neutral voltage is more than 700 V for the fault with a FI of 10 kΩ. On the other hand, the neutral voltage for 11 % changes in loads and USCB switching of 340 kvar are under 100 V. Therefore, the faults can easily be distinguished from LCs and USCB switching by using the threshold voltage of 500 V as indicated in Fig. 7b by a dotted line. In summary, it can be concluded that the threshold of the neutral voltage as 500 V will have the ability to distinguish all SPG faults with FIs up to 10 kΩ and changes in loads up to 11 %.

2) Fault detection and estimation of fault occurrence time: From Fig. 7b, it can be seen that the neutral voltage starts increasing and it takes some time to cross the threshold (500 V) after occurrence of the fault. At this instant, the slope of the neutral voltage is very high and thus, the neutral voltage displacement is used to detect the fault and slope of the neutral voltage to determine the instant at which the fault occurs.

A temporary and a permanent SPG faults with a FI of 100 Ω are applied on phase *A* of feeder 30 as indicated in Fig. 6. The temporary fault is applied at 0.1 s which is cleared at 0.3 s while the permanent fault is applied at 3 s. The neutral voltage and the slope of the neutral voltage are shown in Fig. 8 from where it can be seen that the neutral voltage starts increasing when the permanent fault occurs at 3 s (it is also similar for the temporary fault). From Fig. 8b, it is clear that the neutral voltage exceeds its threshold approximately at 3.006 s whereas the slope of the neutral voltage crosses its threshold at 3.003 s, the instant when the neutral voltage starts increasing. For the test system in Fig. 6, the threshold for the slope of the neutral voltage is considered 100 kV s^{-1} which is set based on the average slope of the neutral voltage for the usual transient of the system. Therefore, the fault is first detected using the slope of the neutral voltage at 3.003 s and confirmed at 3.006 s using the RMS value of the neutral voltage. Thus, the fault occurrence time is estimated as 3.003 s where 3 ms delay appears due to the instrument transformer dynamics and it will be approximately same for all measurements.

3) Identification of fault characteristics: In this case study, the characteristics of SPG faults are also identified, i.e., whether the faults are temporary or permanent. Generally, the neutral voltage increases and remains at a higher value for permanent faults while this voltage returns to its initial steady-state value after the fault is cleared which usually happens for temporary faults. Fig. 8a shows the neutral voltage for both temporary and permanent SPG faults from where it can be seen that the neutral voltage is high during the fault period, i.e., from 0.1 s to 0.3 s. When the fault is cleared at 0.3 s, the neutral voltage start decreasing to its initial value as the fault is temporary. However, the neutral voltage remains high when a permanent fault is applied at 3 s. Therefore, it is clear that the neutral voltage can be used to distinguish the permanent and temporary faults.

Moreover, the characteristic of an intermittent arc fault is different from other faults. Thus, both temporary and permanent arc faults are also simulated to evaluate the performance of the proposed methodology to identify the characteristics of arc faults. The arc fault model presented in [10] is considered in this simulation. The neutral voltage during the faults is shown in Fig. 9a, where a temporary arc fault is applied at 0.5 s which is cleared at 1.5 s and a permanent arc fault is applied at 5 s. In both cases, random FIs between 500 Ω to 10 kΩ (randomly varying during the period of fault) and random arcing voltages of 5 V to 10 V (with 30 % random oscillation) are considered. From Fig. 9a, it is clear that the neutral voltage starts increasing after the occurrence of the temporary faults and returned to the previous value after it is cleared. It can also be seen that the neutral voltage fluctuates around the threshold during the permanent fault. However, the average value of the neutral voltage is higher than V_{th} through which an arc fault can be detected. Therefore, the proposed method is also capable to identify the characteristics of

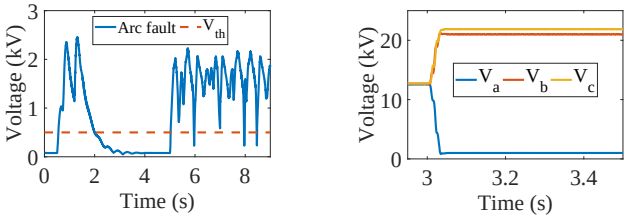

(a) (b)

Fig. 9: a) Neutral voltage (RMS value) for a temporary and a permanent arc faults and b) phase to ground voltages (RMS value) for a permanent non-arc single phase to ground fault.

This article has been accepted for publication in a future issue of this journal, but has not been fully edited. Content may change prior to final publication. Citation information: DOI 10.1109/TPWRD.2018.2799181, IEEE Transactions on Power Delivery

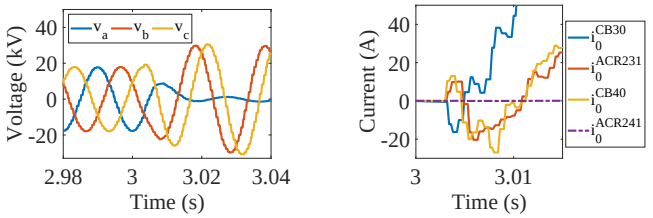

(a) (b)

Fig. 10: a) Phase to ground voltages (instantaneous values) and b) zero-sequence currents (instantaneous values) for a permanent single phase to ground fault.

arc faults.

4) Identification of faulty phase: If the SPG faults are permanent, the proposed technique identifies the faulty phase based on the RMS value of the phase to ground voltages. For a SPG fault, the post-fault phase to ground voltage is less than the pre-fault phase to ground voltage for the faulty phase while it is opposite for other phases. In this case, a permanent fault is applied on phase *A* between node-301 and node-303 at 3 s with a FI of 100 Ω. The RMS values of the phase to ground voltages are shown in Fig. 9b from where it can be seen that the post-fault voltage of the faulty phase (i.e., phase *A*) becomes lower than its pre-fault steady-state value while these post-fault phase voltages are higher for healthy phases (i.e., phase *B* and phase *C*). Thus, phase *A* is identified as the faulty phase.

5) Identification of faulty feeder: In the proposed scheme, the faulty feeder is identified after detecting the faulty phase by observing the changes in the instantaneous zero-sequence current of the feeders and the value of the faulty phase voltage. As mentioned earlier, the nature of change for the zero-sequence current of the feeder and the value of instantaneous faulty phase voltage will be similar for the faulty feeder (i.e., both positive or both negative) while these will be opposite for the healthy feeder. This phenomenon will happen at the instant of occurring a SPG fault. In this paper, these changes are represented in the form of spikes using MM technique through CODO operation. The CODO output for the zero-sequence current in the MM technique is in the form of a positive spike for the faulty feeders while it is negative for the healthy feeder.

Fig. 10 shows the instantaneous values of phase voltages and zero-sequence currents of feeders for the case study discussed in the previous sub-section (VII-A4). From Fig. 10a, it can be seen that the instantaneous value of faulty phase voltage (v_a) is negative when the permanent fault occurs, i.e., at 3 s and at the same time, Fig. 10b shows that the change in zero-sequence currents is negative for CB30 while these are positive for other CB and relays even in the ACR231 which is located on the same feeder but at the downstream. Therefore, the fault occurs in feeder 30 which is before the relay ACR231 as the instantaneous value of faulty phase voltage and the change of zero-sequence currents of CB30 are negative, and the change of zero-sequence currents of ACR231 is positive. The CODO outputs of zero-sequence currents for all CBs and relays are presented in Fig. 11 from where it can be seen that it is positive for CB30 while negative for other CB and relays. Therefore, the CODO outputs indicate that the fault is occurred in the feeder 30 before ACR231 as CB30 is detected the fault and ACR231 is not.

6) Performance evaluation of the proposed method under different compensation levels: Simulation results, so far presented in this paper, are fully obtained for the compensated system. As the system does not always run in the compensated condition (i.e., there are chances to operate the system either in over or under compensated conditions) it is important to analyze the performance of the proposed scheme under different CLs. In the proposed method, there are several voltages and current signals are used. Among these, the neutral voltage and zero-sequence current are mostly affected by the CL which also affects the performance of the proposed scheme. In the over or under compensated system, the neutral voltage will be smaller during faults as compared with the fully compensated system. However, the neutral voltage will still be higher than the threshold if the system is over or under compensated in a reasonable range. If the system is extremely over or under compensated, it will act as a non-RG system. However, the fault detection in a non-RG system is beyond the scope of this paper. Fig. 12a shows the neutral voltage for a SPG fault with a FI of 1 kΩ under different CL. Form this figure, it is clear that the neutral voltage for a fault in over and under compensated system is less than the neutral voltage in fully compensated system. However, the neutral voltage is reasonably high to detect 1 kΩ faults for more than 30% over or under compensated system.

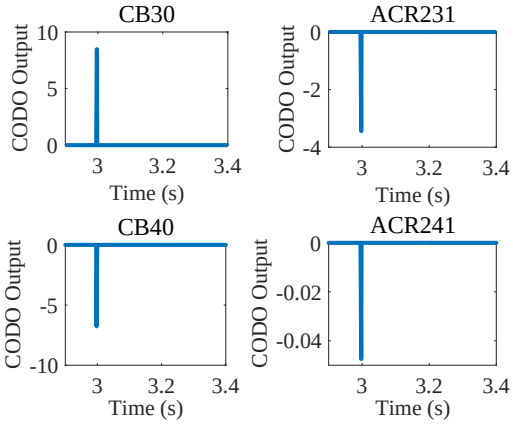

Fig. 11: CODO output of zero-sequence currents for a permanent single phase to ground fault.

Moreover, the magnitude of the zero-sequence current varies under different CLs during a SPG fault. However, the initial transient of zero-sequence current is only used in the proposed method for identifying the faulty feeder which does not depend on the CL as the system takes some times to start the compensation. A SPG fault with a FI of 100 Ω is simulated to justify it. Zero-sequence currents for the fault under different CL is shown in Fig. 12b where faults are applied at 0.1 s. From this figure, it can be seen that the initial transients of zero-sequence currents for all cases are same and their magnitudes start changing when the compensation starts. Therefore, it is clear that there are no effects of the CL to identify the faulty feeder with the proposed method.

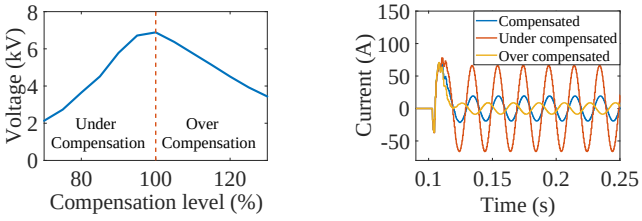

(a) Neutral voltage (b) Zero-sequence currents

Fig. 12: Neutral voltage and zero-sequence currents for a single phase to ground fault under different compensation levels.

This article has been accepted for publication in a future issue of this journal, but has not been fully edited. Content may change prior to final publication. Citation information: DOI 10.1109/TPWRD.2018.2799181, IEEE Transactions on Power Delivery

TABLE I: Case studies for the test system based on a practical system

Cases					Simulation Outputs								
Case no.	FL (area)	FI (kΩ)	FIA (deg.)	CL (%)	FDD (ms)	Nature of Fault	Faulty phase	FDNV	FIFDD				
									CB30	ACR231	ACR233	CB40	ACR241
1	ACR233	10	30	90	14	Permanent	A	**Yes**	**Yes**	**Yes**	**Yes**	No	No
2	ACR231	0.1	110	110	10	Temporary	C	**Yes**	**Yes**	**Yes**	No	No	No
3	CB30	3	10	100	13	Permanent	C	**Yes**	**Yes**	No	No	No	No
4	CB40	0.001	80	80	9	Temporary	A	**Yes**	No	No	No	**Yes**	No
5	ACR241	0.5	200	105	12	Permanent	B	**Yes**	No	No	No	**Yes**	**Yes**

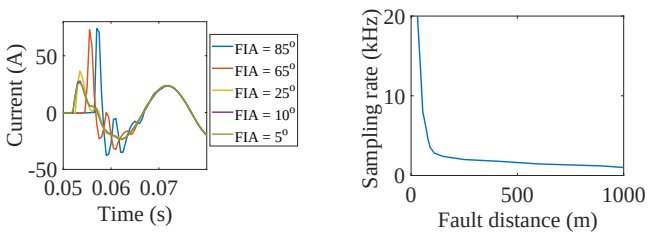

(a) (b)

Fig. 13: a) Zero-sequence current for different fault inception angle and b) the requirement of sampling rate with respect to fault distance.

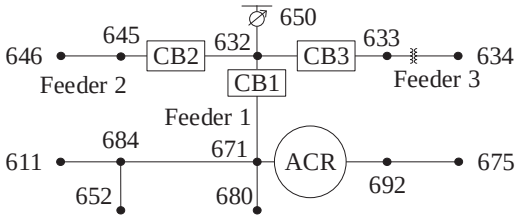

Fig. 14: IEEE 13-node test system.

7) Performance evaluation of the proposed method under different fault inception angles: In the proposed method, the faulty feeder is identified using the initial transient of the zero-sequence current. However, the amplitude of the transient component of the zero-sequence current varies with the FIA which may affect the identification of the faulty feeder. The amplitude of the first transient will be small for the FIAs close to zero or integer multiplication of $\pm 180^\circ$ and it will be high for the FIAs close to odd multiplication of $\pm 90^\circ$. Fig. 13a shows the zero-sequence current for a SPG fault with a FI of $1\ \mathrm{k}\Omega$ under different FIAs from where it can be seen that the amplitude of the first transient is small for the lower value of the FIA. However, the value of the zero-sequence current for a FI of $1\ \mathrm{k}\Omega$ with a FIA of 5° is reasonable to detect by a zero-sequence instrument transformer available in the market. Anyway, the magnitude of the zero-sequence current might vary from system to system depending on the voltage level and FI. Therefore, the magnitude of zero-sequence currents for some faults with FIA very close to zero or integer multiplication of $\pm 180^\circ$ will be very small to detect.

Finally, it can be concluded that the approach presented in this paper has the ability to detect SPG faults as well as distinguish faults from LCs and USCB switching, and identify the faulty phase and feeder. Moreover, the proposed scheme is able to differentiate the permanent and temporary faults. However, the accuracy of the proposed method to identify the faulty feeder depends on the sampling rate of the fault signals (especially, the zero-sequence current). The requirement of the sampling rate depends on the distance of the fault from the relay. For the fault closer to a relay, the oscillation (transient) frequency of the zero-sequence current signal will be higher as the inductive impedance of the line between relay and FL will be smaller. Therefore, the higher sampling rate is required to identify the faulty feeder for faults which are closer to the relay. If the sampling rate is lower than twice of the oscillation frequency, the first transient will be missed out and the relay may make a wrong decision. Several faults are simulated in different locations and the requirement of sampling rate with respect to the distance of faults from the relay is shown in Fig. 13b. From this figure, it is clear that $2\ \mathrm{kHz}$ sampling rate is enough to identify the faulty feeder for the faults which are more than $150\ \mathrm{m}$ away from the relay and higher sampling rate is required for faults closer to the relay.

Apart from the above FL and FI, the simulations are also carried out by considering faults at different locations with different FI, FIA, and CL. Some of the case studies from simulations are summarized in Table I. The fault detection delay (FDD), nature of the fault, faulty phase, fault detection using neutral voltage (FDNV), and fault indication by fault detection devices (FIFDD) in both substation and field levels are shown in Table I for each case studies. Here, FDD is the time delay considering the dynamics of the CTs and PTs, and the speed of the processor (it is assumed that the speed of the modern processor is high enough and delays are approximately $1-2\ \mathrm{ms}$). From the table, it is clear that the proposed method is able to detect any fault within $15\ \mathrm{ms}$ of fault occurrence. Also, it can identify the nature of the fault and faulty phase. The last four columns in Table I are used to show the CBs or ACRs which are detecting these faults from where it is clear that all CBs and ACRs in the upstream of the fault can detect fault. Therefore, the faulty area of a long feeder can easily be identified using a time delay between the CB and ACRs. Thus, it can be summarized that the proposed approach is capable to detect faults at any location within the system with the FI up to $10\ \mathrm{k}\Omega$ within $15\ \mathrm{ms}$. The effectiveness of the proposed scheme is also evaluated on an IEEE test system as discussed in the following subsection.

B. Performance Analysis on an IEEE 13-node Test System

The proposed technique in this paper is also verified on the IEEE 13-node test system $(4.16\ \mathrm{kV})$ test system as shown in Fig. 14. Similar cases, as discussed in the previous subsection, are used to evaluate the effectiveness of the proposed scheme. The results from several case studies are presented in Table II where SPG faults are applied on different parts of the test system shown in Fig. 14. From the simulation results in Table II, it is clear that the proposed technique has the ability to detect faults at any location within the system with the FI up to $10\ \mathrm{k}\Omega$.

C. Performance Comparison with Existing Technique

The performance of the proposed technique has been compared with some existing techniques. The performance comparison is summarized in Table III where NA means not applicable and NG represents not given. In Table III, the limitations are marked in bolded red color. At first, the proposed scheme is compared with existing methods which consider RG (CRG). The proposed

This article has been accepted for publication in a future issue of this journal, but has not been fully edited. Content may change prior to final publication. Citation information: DOI 10.1109/TPWRD.2018.2799181, IEEE Transactions on Power Delivery

TABLE II: Case studies for IEEE 13-node test system

Cases					Simulation Outputs							
Case no.	FL (area)	FI (kΩ)	FIA (deg.)	CL (%)	FDD (ms)	Nature of Fault	Faulty phase	FDNV	FIFDD			
									CB1	ACR	CB2	CB3
1	ACR	0.01	120	100	9	Permanent	B	**Yes**	**Yes**	**Yes**	No	No
2	CB1	0.5	50	80	10	Permanent	C	**Yes**	**Yes**	No	No	No
3	CB1	10	10	105	12	Temporary	A	**Yes**	**Yes**	No	No	No
4	CB2	1	110	70	11	Permanent	A	**Yes**	No	No	**Yes**	No
5	CB3	0.3	200	110	9	Temporary	C	**Yes**	No	No	No	**Yes**

TABLE III: Performance comparison

Method	CRG	FDCF	CAFDCF	FDA (%)	FDTW (ms)	DNP
Proposed	Yes	Yes	No	95.5	15	No
Ref [14]	Yes	Yes	**Yes**	NG	20	No
Ref [13]	Yes	Yes	**Yes**	NG	NG	**Yes**
Ref [12]	Yes	Yes	**Yes**	NG	NG	No
Ref [10]	**No**	**No**	NA	NG	1000	No
Ref [9]	**No**	**No**	NA	93.5	NG	No
Ref [7]	**No**	**No**	NA	NG	NG	No

scheme is then benchmarked against the fault detection capability within the feeder (FDCF) as well as with the same based on the communication, i.e., the communication-assisted fault detection capability within the feeder (CAFDCF). In the 5^{th} column, the fault detection accuracy (FDA) of each method is compared where the FDA is calculated based on the following equation:

$$FDA = \frac{FD + HC}{FD + HC + MF + ND} \; X \; 100\% \qquad (17)$$

where FD is the number of detected faults (actual faults), HC is the number of other disturbances which do not detect as a fault, MF is the number of other disturbance which detected as a fault, and ND is the number of faults not detected. In the next column, the fault detection time windows (FDTWs) for different methods are compared where FDTW is the time range of faults signals required to complete the critical part of the detection process. Finally, methods are compared based on the dependency on the network parameter (DNP) such as the number of feeders in the system. Table III shows that the proposed method is superior to other existing methods to detect faults and identify faulty feeders in a RG system.

VIII. Conclusion and Future Work

In this paper, a fault detection algorithm is proposed to detect SPG faults in RG systems. This algorithm has been tested on an IEEE test system as well as a practical test system through simulation studies. From the case studies, it is seen that the proposed technique can detect a fault, identify the faulty phase and feeder within 15 ms. Also, it can distinguish permanent and temporary faults. Moreover, this technique works in a reasonable range of under and over compensated network as well as for different FIAs. The proposed technique does not require communication between CBs and relays as it uses the local voltage and current information to detect faults and identify the faulty feeder. This work can be further improved by considering the capacitive imbalance of the network. Also, this work can be extended for other types of ground faults. In future, the proposed approach will be implemented on different network configurations (e.g., mesh) with renewable energy sources while considering some uncertainties such as noisy data, variations in renewable power generation.

Acknowledgment

The authors would like to thank Martin Cavanagh and other REFCL team members from AusNet Services for their support to conduct this research.

References

[1] J. Ma et al., "A novel line protection scheme for a single phase-to-ground fault based on voltage phase comparison," *IEEE Trans. Power Del.*, vol. 31, no. 5, pp. 2018–2027, Oct. 2016.
[2] E. C. Piesciorovsky and N. N. Schulz, "Fuse relay adaptive overcurrent protection scheme for microgrid with distributed generators," *IET Generation, Transmission Distribution*, vol. 11, no. 2, pp. 540–549, 2017.
[3] F. B. Costa et al., "Overcurrent protection in distribution systems with distributed generation based on the real-time boundary wavelet transform," *IEEE Trans. Power Del.*, vol. 32, no. 1, pp. 462–473, Feb. 2017.
[4] V. C. Nikolaidis et al., "A communication-assisted overcurrent protection scheme for radial distribution systems with distributed generation," *IEEE Trans. Smart Grid*, vol. 7, no. 1, pp. 114–123, Jan. 2016.
[5] T. Marxsen, "REFCL trial: Ignition tests," Marxsen Consulting, Technical Report, 2014.
[6] K. Chen et al., "Fault detection, classification and location for transmission lines and distribution systems: a review on the methods," *High Voltage*, vol. 1, no. 1, pp. 25–33, 2016.
[7] M. Michalik et al., "New ANN-based algorithms for detecting HIFs in multigrounded MV networks," *IEEE Trans. Power Del.*, vol. 23, no. 1, pp. 58–66, Jan. 2008.
[8] Q. H. Alsafasfeh, "Pattern recognition for fault detection, classification, and localization in electrical power systems," Ph.D. dissertation, 2010.
[9] A. Ghaderi et al., "High-impedance fault detection in the distribution network using the time-frequency-based algorithm," *IEEE Trans. Power Del.*, vol. 30, no. 3, pp. 1260–1268, Jun. 2015.
[10] S. Gautam and S. Brahma, "Detection of high impedance fault in power distribution systems using mathematical morphology," *IEEE Trans. Power Syst.*, vol. 28, no. 2, pp. 1226–1234, May 2013.
[11] I. Zamora et al., "New method for detecting low current faults in electrical distribution systems," *IEEE Trans. Power Del.*, vol. 22, no. 4, pp. 2072–2079, Oct. 2007.
[12] K. J. Sagastabeitia et al., "Phase asymmetry: A new parameter for detecting single-phase earth faults in compensated MV networks," *IEEE Trans. Power Del.*, vol. 26, no. 4, pp. 2251–2258, Oct. 2011.
[13] Y. Wang et al., "Faulty feeder detection of single phase-earth fault using grey relation degree in resonant grounding system," *IEEE Trans. Power Del.*, vol. 32, no. 1, pp. 55–61, Feb. 2017.
[14] A. Nikander and P. Jrventausta, "Identification of high-impedance earth faults in neutral isolated or compensated mv networks," *IEEE Trans. Power Del.*, vol. 32, no. 3, pp. 1187–1195, Jun. 2017.
[15] J. Serra, *Image Analysis and Mathematical Morphology*. Orlando, FL, USA: Academic Press, Inc., 1983.
[16] G. Matheron, *Random Sets and Integral Geometry*. New York: Wiley, 1975.
[17] M. A. Barik et al., "Mathematical morphology-based fault detection technique for power distribution systems subjected to resonant grounding," in *IEEE PES General Meeting*, Chicago, USA, Jul. 2017, pp. 1–5.